PATH DEPENDANCY OF THE RICE J-INTEGRAL IN WELD GEOMETRIES

M.H. Bleackley*
R.D. Jones**
A.R. Luxmoore***

A finite element study of the fracture properties of different weld geometries has been conducted by the authors. The assessment of fracture potential has been made using the Rice J-integral, calculated from the average of a number of paths surrounding the crack. For the case of an undermatched weld metal i.e. weld yield stress lower than the parent plate, a detailed study of the various components of the J-integral path was undertaken. This showed that the high strain concentrations produced at the fusion line by the dissimilarity of the yield stress caused small but significant variations in the J-integral taken from paths crossing this boundary. The development of the strain concentrations is examined and also the effect of the stress-strain behaviour.

INTRODUCTION

In designing against the fracture of large welded plates, it is common practice to specify a weld metal with a higher yield stress than the parent plate, so that strain will not concentrate in the welds in areas of high stress concentration, hence reducing the possibility of fracture. High yield weld metals do not have good fracture toughness, and the welding of high strength plates cannot always be done with a weld metal of equal or higher yield stress.

The writers have been involved in a long term finite element study on the fracture behaviour of different weld geometries past general yield. The assessment of fracture potential has been made using both the Rice J-integral and the crack tip opening displacement (COD). Numerically, the Rice J-integral is the most reliable parameter, but it does have limitations when dealing with material boundaries, etc. In the original definition of the integral, Rice (1) proved path independence for nonlinear elastic

* Nuclear Safety Directorate, Warrington, U.K.
** Engineer, BP Engineering, London U.K.
*** Senior Lecturer, Department of Civil Engineering, University College of Swansea, Swansea, U.K.

materials provided no other singularities were included within the integral's domain. A considerable amount of published literature has shown that this result may be transferred to monotonic loading of materials obeying flow or incremental plasticity laws, using methods of numerical analysis.

The presence of boundaries separating materials of different yield stress near the crack tip could cause stress raising effects equivalent to a singularity, and thus invalidate the path independence requirement of the J-integral.

EVALUATION OF THE J-INTEGRAL FROM FINITE ELEMENT COMPUTATIONS

The J-integral can be evaluated in finite element computations by contour integration or compliance calcuations, the first method using the identity

$$J = \int_{\Gamma} (W\, dy - \underline{T} \frac{\partial \underline{u}}{\partial x} ds) \quad \ldots\ldots\ldots\ldots\ldots\ldots\ldots\ldots \quad (1)$$

for evaluation of the integral anticlockwise around a loop finishing either side of the crack lying along the x-axis, where

W = strain energy density
T = traction vector acting outwards on the loop Γ
u = displacement vector

and

ds = element of arc along the loop

Taking a loop through the Gauss points of a finite element mesh using isoparametric elements, with successive points being joined by straight segments, the integral can be approximated by taking average stresses along these segments. The strain energy density is the sum of the elastic and plastic energy densities, and the integral can be written

$$J = \sum_{\Gamma} \left| (\frac{1}{2}\sigma_{ij}\varepsilon_{ij} + \int_{0}^{\bar{\varepsilon}_p} \bar{\sigma} d\bar{\varepsilon}_p) dy - \sigma_{ij} n_i \frac{\partial u}{\partial x} j ds \right| \quad \ldots\ldots\ldots\ldots \quad (2)$$

where $\bar{\sigma}$ and $\bar{\varepsilon}$ are the effective plastic stress and strain respectively, and n_i is the direction cosine of the linear segment.

Compliance methods use the following relation (1)

$$J = - \frac{\partial P}{\partial a} \quad \ldots\ldots\ldots\ldots\ldots \quad (3)$$

where P is the total energy and a is the crack length. This has proved a popular approach for many investigators, but was considered inappropriate for studies of path independence.

WELD GEOMETRIES AND MATERIAL PROPERTIES

Three weld cross-sections were studied, figure 1, with dimensions as shown. Material behaviour was assumed to be represented by a bilinear stress-strain curve, with Young's modulus of 210 kN/mm^2 and Poisson ratio of 0.3 in the elastic range, and a work hardening parameter of 0.466 kN/mm^2. Yield stress of the parent plate was assumed to be variously 0.60 and 1.0 kN/mm^2, with weld metals having yield stresses of the same value (homogenous specimen), 15% higher (overmatched) and 15% lower (undermatched).

Cracks varied in length from a/W=0.1 up to a/W=0.5, with most work concentrating on the shallow cracks. The cracks were all edge cracks situated in the centre of the weld, figure 1. Three loading cases were studied: 3-point and 4 point bending; direct tension.

All computations were carried out under plane strain constraint, representing behaviour of the welds in infinite plates.

PATH DEPENDANCY OF J-INTEGRAL IN WELDS

Use of Closed Loops

In studying variations of the J-integral by finite element methods, the numerical errors due to discretisation can be assessed by computing J-integrals from closed loops in the same general area containing the crack path. Providing these closed loops do not cross a singularity, they should return a zero J-integral, and any finite value will be due to errors in the numerical procedure. Previous experience has shown that, with well graded meshes, closed loop J-values should be no more than 1% of the crack tip J-value at the same loading state. Variations between different paths of the crack tip J-value can be as much as 10% for homogeneous specimens (this assumes very small paths close to the crack tip and paths around specimen boundaries are excluded, as they give large deviations). Hence numerical errors are usually a small part of the variations between different crack tip J-paths.

Computations on Double-V Geometry

A 54 element mesh was designed to represent the cracked specimen half space, figure 2, and this mesh was used to model crack lengths of a/W = 0.147, 0.31 and 0.49. Figure 3 shows the paths selected to calculate the J-integral, with paths 1 to 4 lying entirely in the weld metal, and paths 5 to 8 crossed the fusion line. Paths 9 and 10 were closed loops with path 9 crossing the fusion line, and path 10 lying entirely in the weld metal.

A separate 100 element mesh was used for a shallow crack with a/W = 0.098, but the J-paths were very similar.

Geometry	Paths	a/W	Weld Metal Yield Stress kN/mm	Maximum Variation from Mean of Path. Sets %	Corresponding Equivalent Homogeneous Result for Same a/W Value
BEND 3	A	0.098	0.78	3.8	1.2
	B	0.49	0.78	-5.8	1.7
BEND 4	A	0.49	0.51	3.1	2.8
	B	0.49	0.51	-1.0	-0.9
SENT	A	0.49	0.78	-12.4	-2.6
	B	0.49	0.78	4.1	0.9

TABLE 1 – Variation of Path Sets from the Mean J-Value for Double-V Weld.

In the final analysis, the J-values from paths 1 and 8 were rejected as being too near the crack tips and specimen boundary respectively. A great deal of scatter was observed, and table 1 summarises some of the results. The paths within the weld metal were averaged (paths A), as were those which crossed the fusion line (paths B). The results for homogenous specimens (weld metal and parent plate with same yield stress) at the same a/W values are included to give some indication of the numerical error, as the paths are identical. This is not entirely satisfactory as the different weld yield stress will produce different plastic zones. The largest variation in J-values occurs for paths entirely within the weld metal in specimens subjected to dirct tension (SENT), and this suggests the presence of the fusion line is not significant in comparison with other effects, although the homogenous specimens showed much smaller variations. Path independency was generally more marked with the shallow cracked (a/W = 0.098) SENT specimen, but this result was sensitive to mesh variations.

Closed path 9 produced the largest closed loop J-values (9% of crack tip J-value), and this occurred for the shallow cracks in the SENT specimen, with the shallow crack producing the highest closed loop error for all loading types. However 90% of

all closed loop values were less than 3% of the crack tip J-value.

Investigation of Path Variations by Contour Segmentation

A further investigation of path variations was conducted on shallow cracked (a/W = 0.1) SENT specimens with undermatched weld metal for all three weld geometries. The previous work described in section 4.2 had shown this combination to be the most sensitive for the double V weld.

Three adjacent closed loops P1, P2 and P3 were constructed so as to straddle the fusion boundary, figure 4, such that a fourth closed loop P4 formed the outer envelope, and the J-values give

$$J4 = J1+J2+J3 \quad \ldots\ldots\ldots\ldots\ldots\ldots \quad (4)$$

Providing the mesh is well graded, the values of J1 and J3 should exhibit little numerical error, as their paths are placed entirely within the weld metal and parent plate respectively, and so

$$J4 \approx J2 \quad \ldots\ldots\ldots\ldots\ldots\ldots \quad (5)$$

If J4 >> J1 or J3, then the fusion line is perturbing the continuity of the stress/strain field.

Three separate meshes were used for the double V geometry, so that the effect of mesh grading could be assessed. Two of the three meshes produced identical elastic behaviour, and identical elastic fracture parameters, which agreed closely with published values, and only the results from these two meshes are reported.

Figure 5 shows the variation of J1 to J4 for the two double V meshes, and the results do indicate a discontinuity in the fusion line, although the mesh refinement affects the results considerably. The closed path in the parent plate (P3) produced negligible errors, but the weld metal closed loop produced a larger error, which became constant as loading increased. The fusion line path P2, and hence the total path P4, gave increasing J-values with increasing load, and it would appear that J4 ≈ J2 >> J1 and J3 at large displacements.

The crack tip J-values for the double-V specimen were evaluated around the paths shown in figure 6 (the paths varied slightly between the two meshes). Figure 7 shows the variations obtained, with differences up to 20%, but the two loops contained within the weld metal gave very similar J-values, and the variation of the "weld only" J-values between meshes was less than 5%.

A somewhat similar, but greatly reduced, effect was observed in the single-V geometry. The rectangular strip weld, however, showed no discontinuity effects at the fusion line, and the three geometries are compared by plotting the J-values obtained from a single closed path taken right around a fusion line (evaluated from the Gauss points adjacent to the fusion line), figure 8. The double-V geometry shows a closed loop J-value which is significant compared with discretisation effects, whereas the other two geometries do not.

STRAIN DISTRIBUTIONS IN UNDERMATCHED WELDS

The apparent discontinuity in the double-V fusion line is a direct result of the geometry and degree of undermatching. A detailed study has been made of the stress and strain distributions in uncracked, undermatched weld geometries (2), and this has shown that, once the weld metal yields, the parent plate acts as a rigid insert, and builds up large shearing effects on the fusion flanks as the loading continues. Plastic strain is concentrated within the weld material on these flanks, and increases in strain occur in the region of the fusion line, at the expense of the middle of the weld.

The sudden transition across the fusion line from peak plastic strain to elastic strain produces a discontinuity in the energy density, figure 9 (the changes in stress across the fusion line are much smaller) and this is the cause of the discontinuity in the J-value. The other two weld geometries studied did not produce this sudden change. The centre of the double-V geometry shows similar strain energy densities either side of the fusion line, and the difference is only large on the sloping flanks, where the shearing effects are a maximum.

The strain distribution also explains the rather unusual shape of the J versus displacement curve for the double-V specimen. This is exemplified in figure 10, where the J-value of the three geometries with the same undermatched weld properties are compared with results from homogeneous specimens having yield stresses equivalent to the parent plate and weld metal respectively. The result for the double-V specimen shows a very significant reduction in J-value after general yield, compared with all the other specimens (a similar, but much smaller effect is observed in the single-V behaviour). The crack is situated on the centre line of the weld, and after general yield, the flanks of the fusion boundary sustain nearly all the plastic strain, and the weld metal around the crack shows a very small increase in strain, and hence a correspondingly small increase in the J-value.

RELATION BETWEEN J AND COD

The unusual stress/strain distribution in the double-V geometry cast some doubts on the usefulness of the J-integral as a fracture parameter in this situation. As a simple check, the J-value was plotted against the crack tip COD. The COD was calculated from the numerical results by extending the straight flanks of the crack, and observing their separation at the crack tip, which was, of course, curved. This approximation of the COD has been used previously by one of the writers, and found to be satisfactory.

All geometries gave very similar linear relationships, using average J-values (for the double-V specimen, the average was taken from weld only contours), and agreed with the relation

$$J = t\sigma_y \delta \qquad \ldots\ldots\ldots\ldots\ldots\ldots \quad (6)$$

where t is the constraint factor, and δ is the COD.

For the homogeneous specimens, t=1.24 and using the yield stress of the weld material for the undermatched geometries, the values were t=1.38 (rectangular strip), 1.27 (single-V) and 1.14 (double-V). The latter value is very close to the Von Mises plane strain value of 1.15, where no constraint is provided by the geometry of the specimen, and this is the case for the double-V specimen.

Effect of Material Stress-Strain Curve

In an attempt to compare finite element results with semi-analytic models of weld behaviour, the basic stress-strain curve was changed so as to represent actual material behaviour more closely, and also to study the effect of using a power hardening representation (Ramsberg-Osgood relation) of the stress-strain curve, figure 11.

The computations were repeated for homogeneous specimens only, with the resulting J-values shown in figure 12. The differences produced by different representations of the stress-strain curve are highly significant, and much larger than the variations observed due to J-integral paths crossing the fusion line. The differences can be attributed to the use of effectively different yield and flow stresses. These results emphasise the critical nature of stress-strain representation, and go some way to explaining why large differences are often obtained from nominally identical computations on the nonlinear behaviour of fracture specimens, which is currently being studied as a round robin exercise by the European Group on Fracture.

CONCLUSIONS

The presence of the fusion boundary can produce a discontinuity in the evaluation of the J-integral from a line integral crossing the fusion line. This effect is only significant when using well undermatched weld metal in double-V geometries, where errors of up to 20% have been observed. The discontinuity is associated with large differences in strain energy density either side of the fusion line, just after the weld metal yields, and is associated with the large shearing effects produced by the effectively rigid (unyielded) parent plate pulling on the softer (yielded) weld metal.

No effective discontinuity was observed in either a single-V or rectangular strip welds, compared with the numerical errors involved in calculating the J-integral.

The unusual strain distributions in the double-V specimen also produce a much lower J-value for the same applied displacement than in the single-V and rectangular strip welds. This is probably only true for shallow central edge cracks.

The errors caused by taking path integrals across the fusion line are insignificant compared with the differences obtained from various representaions of the material stress-strain curve, and it is this aspect of numerical work that should receive more attention.

Further work is currently in progress on different degrees of undermatching, and the effects of surface and buried cracks near to and on the fusion lines.

REFERENCES

(1) Rice, J.R. "A Path Independent and the Approximate Analysis of Strain Concentration by Notches and Cracks" (1968) J. Appl. Mech. Vol.35, pp. 379-386.

(2) Bleackley, M.H., Jones, R.D. abd Luxmoore, A.R. To be published.

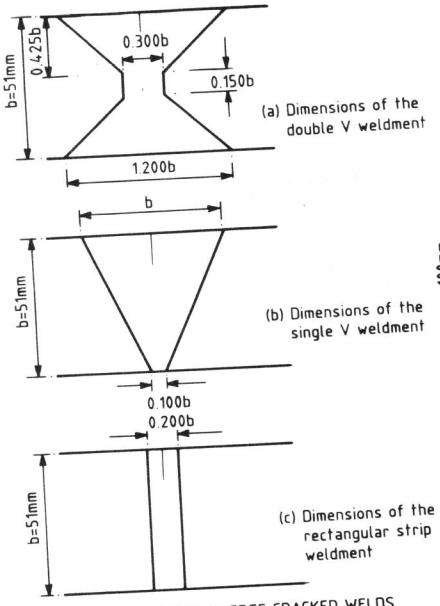

FIGURE 1 GEOMETRIES OF EDGE CRACKED WELDS

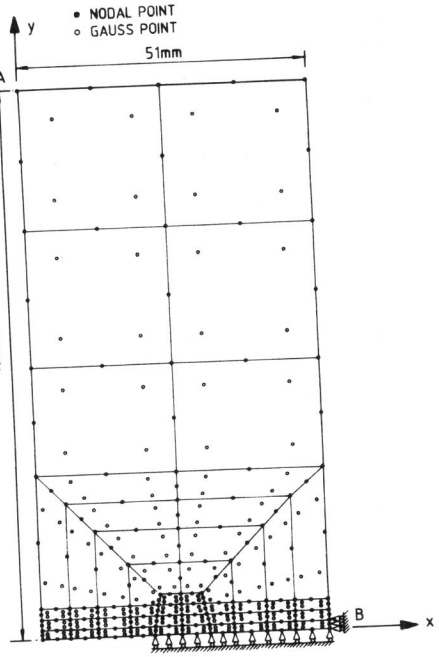

FIGURE 2 54-ELEMENT MESH FOR THE BEND AND SENT SPECIMENS

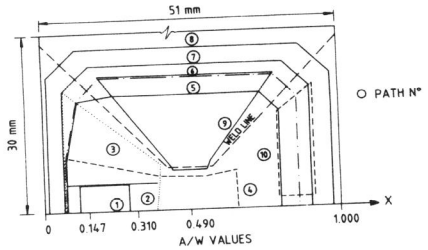

FIGURE 3 DETAILS OF THE J-INTEGRAL PATHS ENCOMPASSING THE CRACK-TIP OF THE DOUBLE V GEOMETRY FOR A/W = 0.147 , 0.31 , 0.49 (54-ELEMENT MESH)

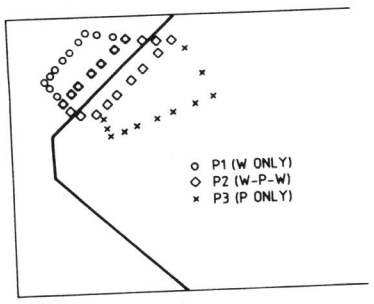

FIGURE 4 CLOSED PATH DISCONTINUITY TEST(MESH A) SHOWING THREE SUB-CONTOURS

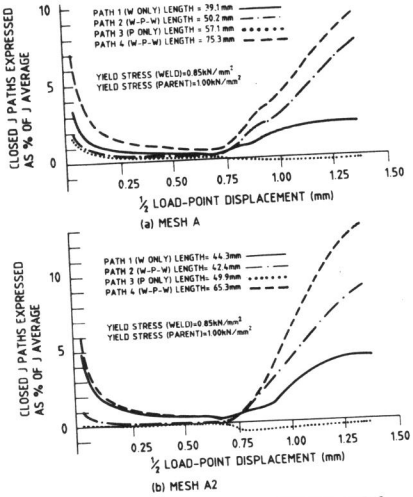

FIGURE 5 VARIATION OF CLOSED J-INTEGRAL PATHS (% OF J AVERAGE) AGAINST DISPLACEMENT FOR TWO MESHES

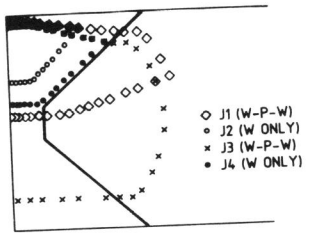

FIGURE 6 INDIVIDUAL OPEN J CONTOUR PATHS FOR MESH A

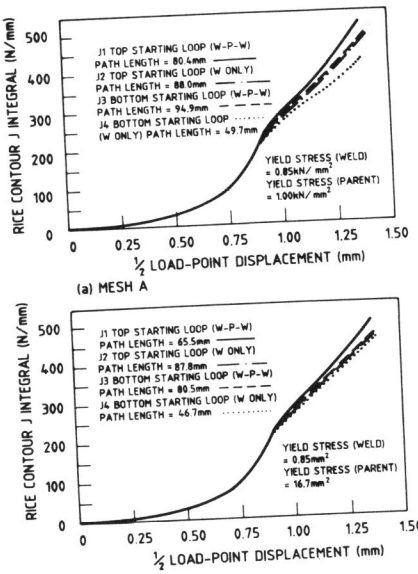

FIGURE 7 VARIATION OF J INTEGRAL WITH APPLIED DISPLACEMENT FOR THE TWO MESHES MODELLING THE DOUBLE V NOTCH SPECIMEN

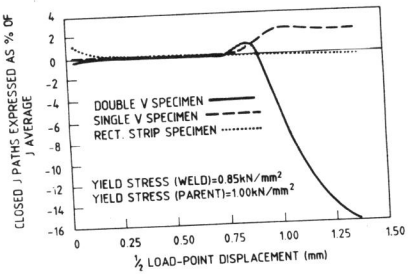

FIGURE 8 ASSESSMENT OF THE NUMERICAL ERROR INCURRED FOR THE THREE WELD GEOMETRIES FROM CLOSED CONTOUR PATH ENCLOSING FUSION LINES

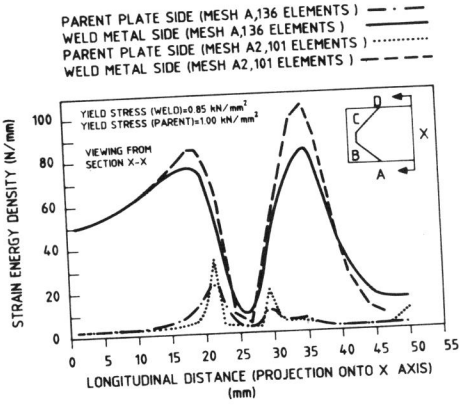

FIGURE 9 COMPARISON OF STRAIN ENERGY DENSITY VALUES EITHER SIDE OF THE FUSION LINE FOR MESHES A AND A2

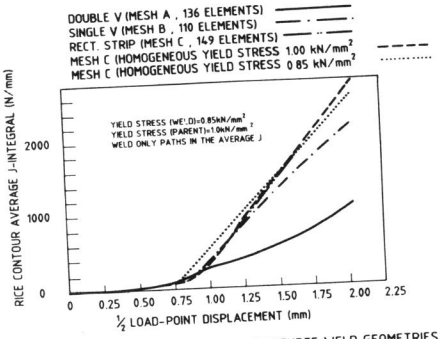

FIGURE 10 COMPARISON BETWEEN THE THREE WELD GEOMETRIES AND HOMOGENEOUS SPECIMENS OF AVERAGE J-INTEGRAL AGAINST LOAD POINT DISPLACEMENT FOR SHALLOW CRACKED SPECIMENS (a/W=0.1)

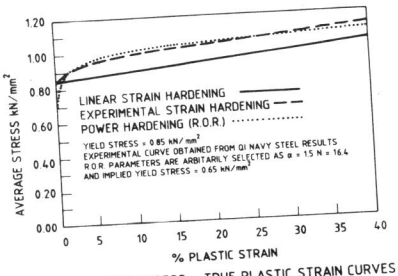

FIGURE 11 TRUE STRESS - TRUE PLASTIC STRAIN CURVES FOR THE HIGH YIELD IDEALISED MATERIAL

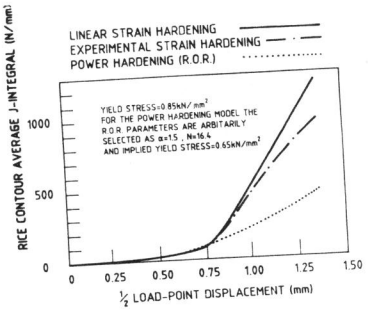

FIGURE 12 VARIATION OF J INTEGRAL WITH DISPLACEMENT FOR A HOMOGENEOUS SENT SPECIMEN